Comments on Inorganic Chemistry
Publication details, including instructions for authors and subscription information:
http://www.informaworld.com/smpp/title~content=t713455155

Redox Changes in Mononuclear Copper Complexes Containing the N_2S_2 Donor Set. Electrochemical Parameters as a Probe of the Structural Features

Piero Zanello[a]
[a] Dipartimento di Chimica, Università di Siena, Siena, Italy

To cite this Article Zanello, Piero(1988) 'Redox Changes in Mononuclear Copper Complexes Containing the N_2S_2 Donor Set. Electrochemical Parameters as a Probe of the Structural Features', Comments on Inorganic Chemistry, 8: 1, 45 — 78
To link to this Article: DOI: 10.1080/02603598808048672
URL: http://dx.doi.org/10.1080/02603598808048672

Redox Changes in Mononuclear Copper Complexes Containing the N_2S_2 Donor Set. Electrochemical Parameters as a Probe of the Structural Features

PIERO ZANELLO
Dipartimento di Chimica,
Università di Siena,
53100 Siena,
Italy

The electrochemical behavior of a wide series of CuN_2S_2 complexes is examined. The stereodynamic copper(II)/copper(I) redox change is by far the most important one in this type of derivative, which in many cases constitutes a valid model for blue copper proteins. Both the thermodynamic and kinetic aspects of the electrode processes are correlated to the stereochemical reorganizations accompanying the redox changes, as well as to the electronic effects of the ligands.

Key Words: *electrochemistry of mononuclear CuN_2S_2 complexes, structure–redox relationships in biomimetic models of copper proteins*

INTRODUCTION

The central role of the Cu(II)/Cu(I) redox couple in enzymes involved in biological electron-transfer processes has stimulated a great deal of work towards the characterization of low molecular weight copper complexes with coordination spheres able to model those now known for copper-containing proteins.[1–4]

Dating from the X-ray structural ascertainment of the distorted tetrahedral geometry of the copper center in poplar plastocyanin,

Comments Inorg. Chem.
1988, Vol. 8, Nos. 1 & 2, pp. 45–78
Reprints available directly from the publisher
Photocopying permitted by license only

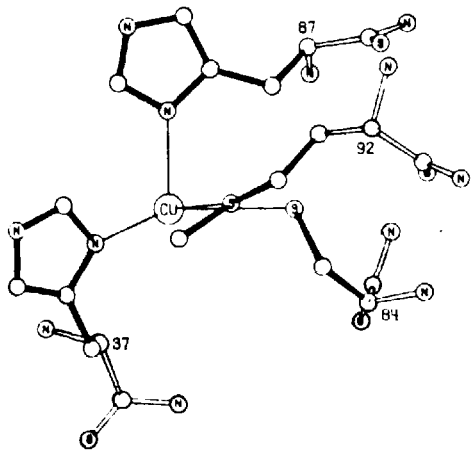

FIGURE 1 Perspective view of the copper center in poplar plastocyanin and relevant bond distances (from Refs. 5, 6).

Fig. 1,[5,6] the chromophore CuN_2S_2 has assumed more and more relevancy in mimicking the active site of Type I (or "blue") copper proteins, even if this inner coordination is not the only one present in such proteins.[1–4,7,8]

Among the distinctive features of this group of proteins,[1–4] we are interested here in giving evidence of their rather high Cu^{II}/Cu^{I} reduction potentials (from 0 to +0.6 V, versus S.C.E.).[9] If one considers that the aquocopper(II/I) couple is located at −0.08 V (versus S.C.E.), it can be deduced that in these protein sites the access to the copper(I) state is markedly facilitated. Two main features have been disputed[10] to be at the origin of (but really cooperative for the attainment of) these high potentials: (i) the coordination of copper to soft sulfur atoms, which stabilize the copper(I) state because of their high π-acceptor ability; (ii) the distorted tetrahedral geometry of the inner-coordination sphere of the copper(II) ion forced by the protein superstructure, which, resulting in a small stereochemical reorganization upon one-electron addition, thermodynamically favors the reduction step. In this connection it must be taken into account that, in the absence of steric constraints, the copper(II) ion commonly adopts six-coordinate octahedral or rhombic, five-coordinate square-pyramidal or

trigonal-bipyramidal, or four-coordinate square-planar geometries, whereas the copper(I) ion prefers the four-coordinate tetrahedral assembly.

We underline that structural reorganizations accompanying redox changes are made evident not only by the thermodynamic standard electrode potentials, but also by the kinetic aspects of the electrode processes. In fact, if one can discard the presence of interfacial phenomena, the rate of the heterogeneous electron transfer between the electrode and a metal complex is largely conditioned by the occurrence of significant structural rearrangements within the complex, which, raising the activation barrier to the charge transfer, slow down the rate of the redox change.[11]

In an attempt to give a brief classification of the different ligand designs used to synthesize CuN_2S_2 compounds, let us divide the complexes according to the Scheme I (L = N or S):

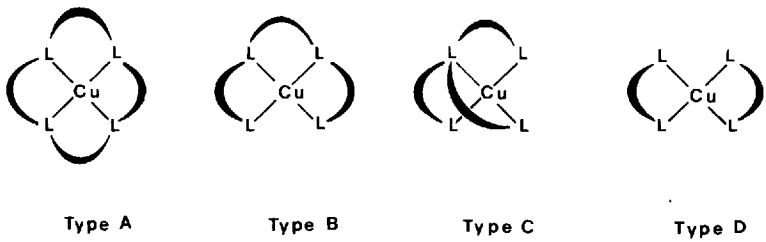

SCHEME I

1. Type A Complexes

The redox behavior of the macrocyclic copper(II) complexes **1**–**9**, schematized in Chart I, has been investigated by electrochemical techniques.[12–15]

Notice that in the series **1**–**4**, the increase of the ring size occurs under a *cis*-arrangement of the heteroatoms, whereas in the series **5**–**9** the heteroatoms have a *trans*-arrangement.

Figure 2 shows the typical cyclic voltammetric response relative to the copper(II)/copper(I) reduction step exhibited by these complexes. It refers to **2** in acetonitrile solution.[14]

Usually these complexes also display a second reduction process, corresponding to the one-electron reduction copper(I)/copper(0), irreversible in nature because complicated by fast decomplexation

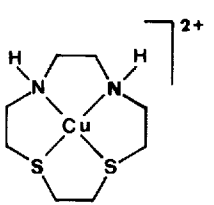

1

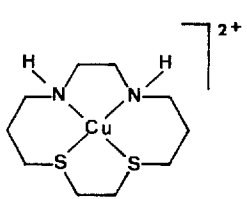

2

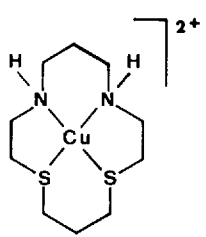

3

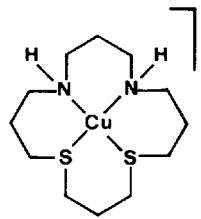

4

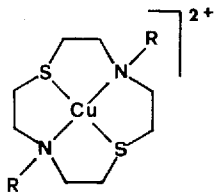

R = H 5
R = CH_3 6
R = $CH_2C_6H_5$ 7

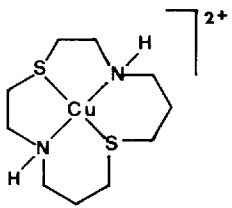

8

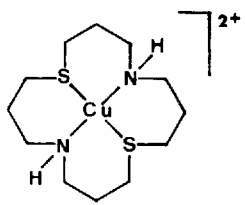

9

CHART I

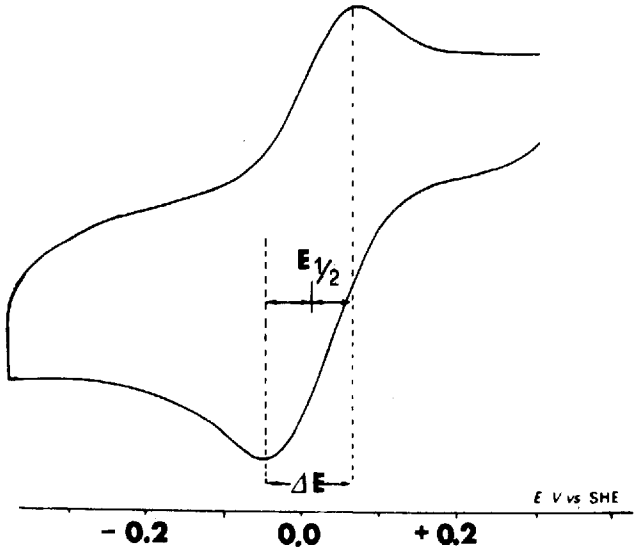

FIGURE 2 Cyclic voltammogram recorded at a platinum electrode on a MeCN solution of **2**. Scan rate 0.01 Vs^{-1} (from Ref. 14).

of the copper metal.[13] It is hence evident that the more interesting redox change is the chemically reversible copper(II)/copper(I) step.

Since we are interested in elucidating structural–electron transfer relationships, we can take advantage in principle of two electrochemical parameters outlined in the introduction: the relative location of the formal electrode potentials for the Cu^{II}/Cu^{I} couple; the extent of electrochemical reversibility, as measured by the peak-to-peak separation of the cyclic voltammetric response (ΔE_p), taking into account that a purely reversible one-electron charge transfer (involving no significant structural reorganization) is characterized by a ΔE_p of 59 mV.[16] Both these parameters for all the complexes **1–9** are summarized in Table I. It is however commonly wise to regard routinely obtained values of ΔE_p greater than 59 mV as indicative of the occurrence of stereochemical reorganizations accompanying the one-electron redox change, without drawing conclusions about the extent of such reorganizations, since this parameter contains a number of other microscopic contributions.[11]

Lacking crystal structure data, we can speculate about the redox

TABLE I

Redox potentials (in volts, vs. S.C.E.) for the copper(II)/copper(I) reduction of the macrocyclic copper(II) complexes **1–11** (schematized in Charts I, II)

Complex	$E^{0'}_{Cu^{II}/Cu^{I}}$	ΔE_p (mV)	Solvent	Ref.
1	−0.08	84[a]	MeCN	14
1	−0.12	–	H_2O	15
2	−0.23	120[a]	MeCN	14
2	−0.16	–	H_2O	15
2	−0.17	181[b]	H_2O	12
3	−0.09	153[b]	H_2O	12
4	+0.23	160[a]	MeCN	14
4	+0.18	–	H_2O	15
5	−0.11	88[a]	MeCN	14
5	−0.07	–	H_2O	15
5	+0.14	70[c]	PC	13
5	−0.10	70[c]	H_2O	13
6	+0.23	60[c]	PC	13
6	−0.02	70[c]	H_2O	13
7	+0.31	66[c]	PC	13
8	−0.07	148[a]	MeCN	14
8	+0.02	–	H_2O	15
9	+0.24	146[a]	MeCN	14
9	+0.16	–	H_2O	15
10	+0.26	88[b]	MeCN	18
10	+0.08	–	DMF	18
11	+0.29	–	MeCN	18
11	+0.08	–	DMF	18

[a]Scan rates from 0.01 to 0.03 Vs^{-1}.
[b]Scan rate not specified.
[c]Scan rate < 0.1 Vs^{-1}.

potentials. As shown in Fig. 3, both in the *cis*- and *trans*-arrangement the access to copper(I) species is significantly facilitated when the cavity size increases from 14- to 16-membered rings. In analogy with the similar tetraaza-copper(II) macrocycles,[17] this result has to be ascribed to the fact that the 14-membered ligands are just able to locate the copper(II) ion with the strongest in-plane interactions, so that the rearrangement to the tetrahedral or pseudo-tetrahedral copper(I) geometry requires a considerable amount of energy. On the contrary, the enlargement of the cavity size, diminishing these in-plane interactions, makes the complex more flexible, so that the reorganization to a tetrahedral geometry is favored with respect to the previous cases. Concerning the 12-

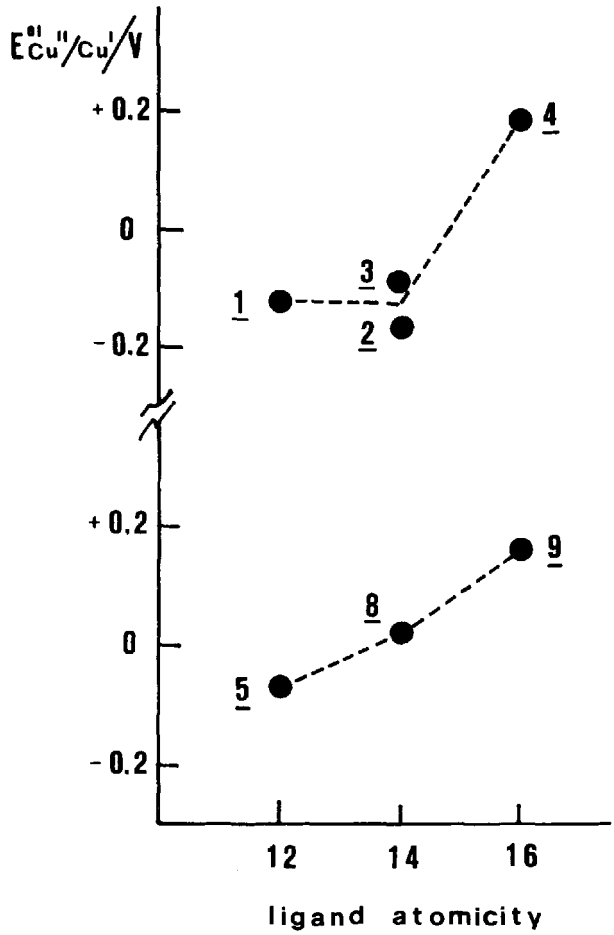

FIGURE 3 Plot of the $E^{0'}_{Cu(II)/Cu(I)}$ values (aqueous solution) of the macrocyclic complexes schematized in Chart I vs. the number of atoms (C,N,S) in the different rings.

membered rings, since their small cavity is unable to give rise to a square planar assembly, they are expected to destabilize the copper(II) species. This is not unequivocally proven.

A further consideration has to be taken into account for compounds **6** and **7**. Since methyl and benzyl substituents are more

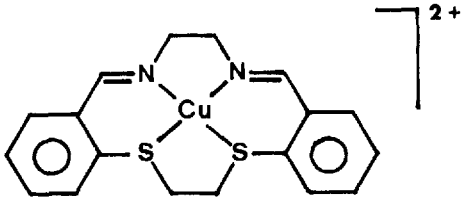

10

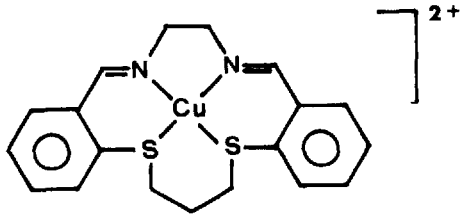

11

CHART II

electron-donating than the hydrogen atoms, one would have expected their electronic effects to disfavor access to the copper(I). Really the redox potentials go in the opposite side. We attribute this to the fact that such bulky substituents induce distortions from the planarity with respect to the unsubstituted copper(II) complex, thus stabilizing the copper(I) state.

The macrocyclic copper(II) complexes **10**, **11**, schematized in Chart II, belong to the type A complexes, too. Figure 4 shows the quasireversible copper(II)/copper(I) reduction exhibited by **10** in cyclic voltammetry.[18] The redox potentials for both **10** and **11** are reported in Table I. Since spectroscopic evidence assigns a planar geometry to these complexes,[18] the rather high potentials with respect to the same-membered complex **2** might be in good part ascribed to the electronic effects of the ligand unsaturation, rather than to increased flexibility.

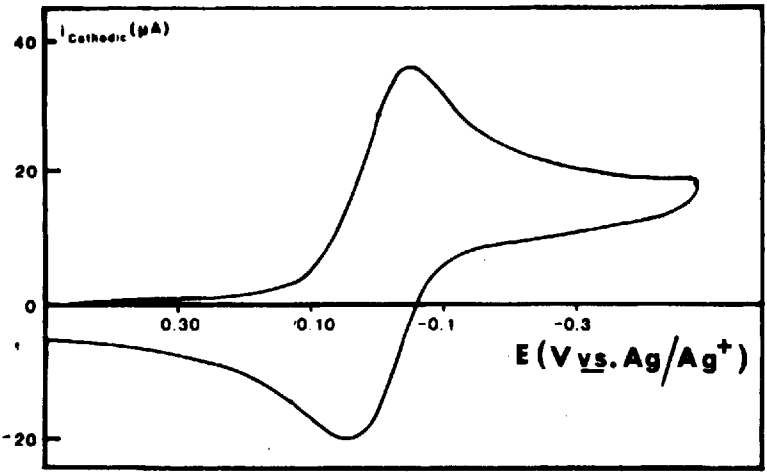

FIGURE 4 Cyclic voltammogram recorded at a platinum electrode on a MeCN solution of **10** (from Ref. 18).

2. Type B Complexes

Most CuN_2S_2 derivatives belong to the open-chain type B complexes.

Let us start with the diaminodithiaethers **12–18**, schematized in Chart III. All these complexes undergo the copper(II)/copper(I) reduction through a quasireversible charge transfer. Table II summarizes the relevant redox potentials. Comparison with the redox potentials of the corresponding macrocycles (Table I) shows that the open-chain complexes are easily reducible (on the average from 100 to 200 mV). This lower reorganizational barrier to the tetrahedral copper(I) geometry has to be attributed to the reduced rigidity of the open-chain ligands, which allows either the copper(II) ion to assume geometries more distorted from planarity than in the corresponding macrocycles, or the copper(I) ion to assume easily its tetrahedral geometry.

In order to evaluate the effect of substituting nitrogen atoms for sulfur atoms, notice that the copper(II)/copper(I) reduction of the tetraaza analogues of **16** and **18** is shifted (in acetonitrile solution) towards negative potential values of about 600 mV.[22]

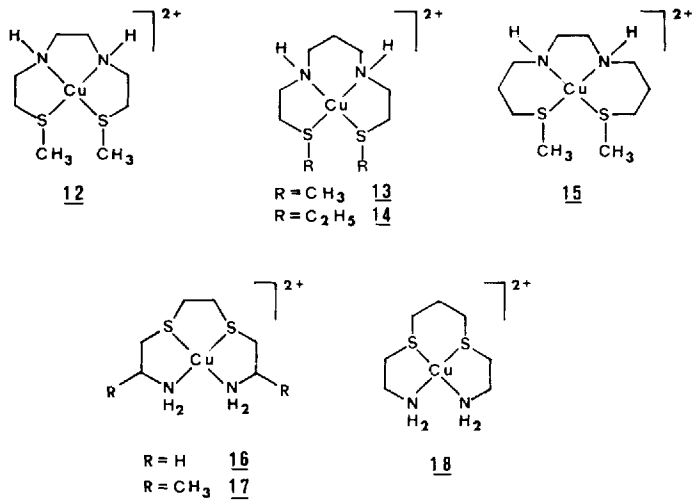

CHART III

Consider now the complexes **19–30** schematized in Chart IV, which exhibit different degrees of unsaturation on the ligands and a N⌒N bridge connecting the two wings. Figure 5 shows the cyclic voltammogram exhibited by **19** in acetonitrile solution.[23] Apart

TABLE II

Redox potentials (in volts, vs. S.C.E.) for the copper(II)/copper(I) couple of the complexes **12–18** (schematized in Chart III)

Complex	$E^{0'}_{Cu^{II}/Cu^{I}}$	ΔE_p (mV)	Solvent	Ref.
12	+0.04	63[a]	H_2O	19
13	−0.01	95[a]	H_2O	19
14	−0.01	152[b]	H_2O	12
14	+0.01	–	aqueous-80% MeOH	20
15	+0.02	63[a]	H_2O	19
16	+0.05	96[b]	H_2O	12
16	+0.12	–	aqueous-80% MeOH	20
17	−0.06[c]	–	MeCN	21
18	+0.07	–	aqueous-80% MeOH	12,20

[a]Scan rates from 0.01 to 0.03 Vs^{-1}.
[b]Scan rate not specified.
[c]Peak potential value for irreversible process.

from both the cathodic and anodic two-electron irreversible processes B and L, likely ligand centered, it is evident that in the cyclic voltammetric time scale the copper(II) complex can undergo the uncomplicated anodic copper(II)/copper(III) oxidation and cathodic copper(II)/copper(I) reduction. However in the longer times of electrolysis the copper(III) species proved to be unstable.

While the anodic oxidation to copper(III) is rarely evident, the chemical reversibility of the copper(II)/copper(I) couple is a common feature of these complexes, too.

A glance at Table III immediately allows us to observe that the copper(II)/copper(I) redox potentials span from quite negative potentials (-1.18 V for **20** in MeCN) to rather positive potentials ($+0.42$ V for **23** in MeCN). This positive shift (of about 1.6 V) must be in part due to electronic effects of the ligands (the presence of functions which decrease the electron density on the metal, so favoring access to copper(I)), and in part to stereochemistries of copper(II) complexes approaching more and more closely the pseudotetrahedral assembly expected for copper(I) complexes.

As shown in Fig. 6, the crystal structure of **19** reveals that the inner-coordination of the copper(II) ion is distorted planar, the low tetrahedral distortion being evaluable by a dihedral angle of 30.0° between the planes defined by the CuN_2 atoms and the CuS_2 atoms, respectively.[29] The same extent of tetrahedral distortion is grossly present in **28**; in fact the twist angle between the CuN_2 and CuS_2 planes, Fig. 7, is 20.0°.[30] Unexpectedly, the complex **22**, which possesses a square planar CuN_2S_2 moiety,[31] is more easily reducible than **19** and **28**. It is hence evident that global electronic effects predominate over stereochemical factors.

Contrary to what is expected, **20**, the flexibility of which should accommodate more easily a pseudotetrahedral copper(I) center, reduces at potentials more negative than **19** does. On the other hand, in the complexes **29** and **30**, congeners of **28**, increasing the methylenic chain strengthens the tetrahedral distortion (the twist angle increases to 52.8° and 57.1°, respectively)[28]; correspondingly the reduction potentials shift to less negative values.

An analogous trend towards progressive tetrahedral distortion with the $\overset{\frown}{N\ \ N}$ carbon chain length has been inferred by spectroscopic measurements concerning the complexes **24–26**.[32] In nice agreement, the redox potentials shift towards positive potentials.

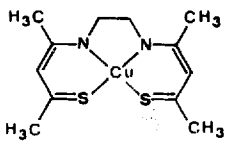

19

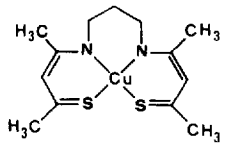

20

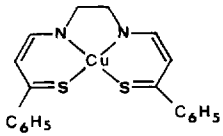

21

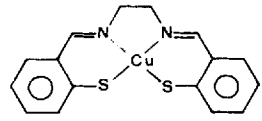

22

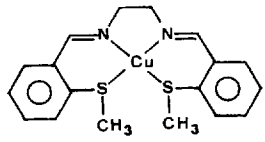

23

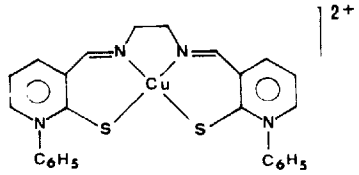

24

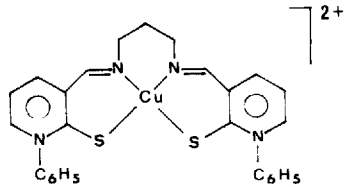

25

CHART IV

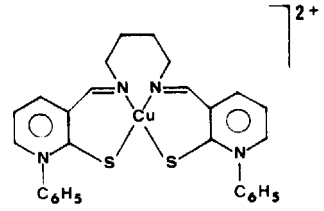

26

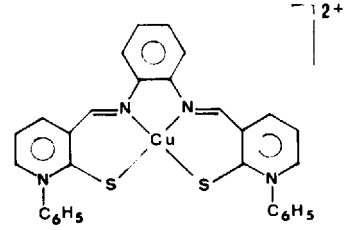

27

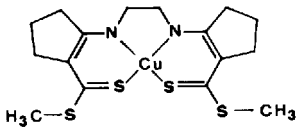

28

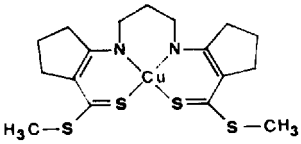

29

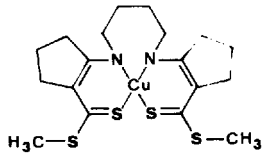

30

CHART IV (*continued*)

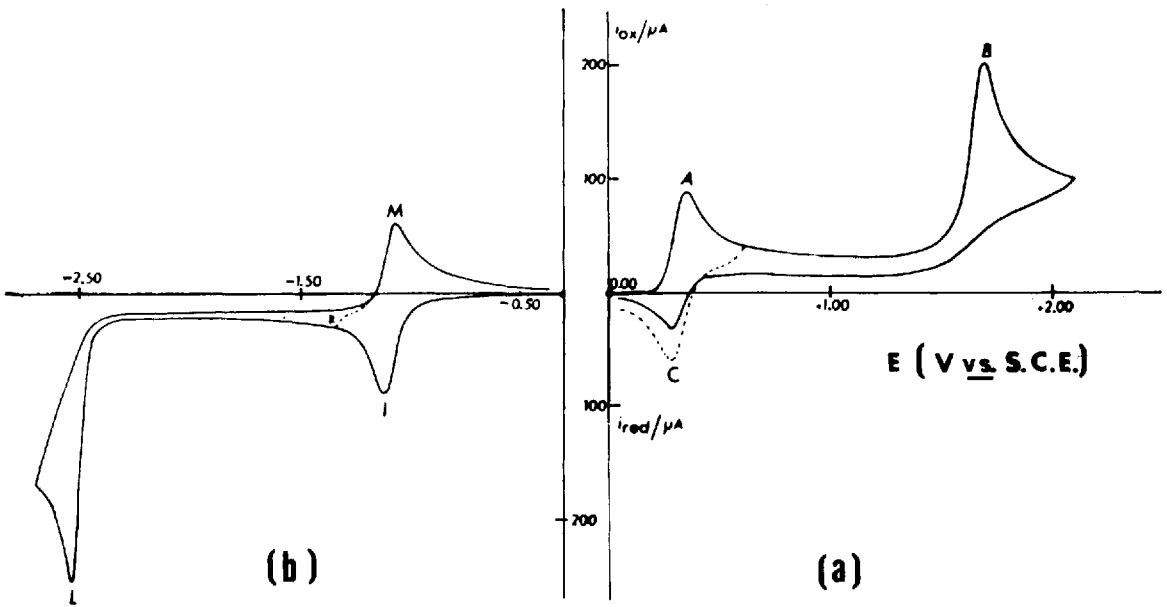

FIGURE 5 Cyclic voltammograms recorded on MeCN solutions of **19**. (a) Platinum working electrode; (b) mercury working electrode. Scan rate 0.2 Vs^{-1} (from Ref. 23).

TABLE III

Standard electrode potentials (in volts, vs. S.C.E.) for the redox changes exhibited by the copper(II) complexes **19–30** (schematized in Chart IV)

Complex	$E^{0'}_{Cu^{II}/Cu^{I}}$	ΔE_p (mV)	$E^{0'}_{Cu^{III}/Cu^{II}}$	ΔE_p (mV)	Solvent	Ref.
19	−1.12	70[a]	+0.27	65[a]	MeCN	23
19	−1.09	80[b]	−0.47	80[b]	MeCN	24
19	−1.07	68[c]	–	–	DMF	25
20	−1.18	85[b]	+0.35	65[b]	MeCN	24
21	−0.87	–	–	–	DMF	25
22	−0.83	–	–	–	DMF	25
23	+0.42	90[d]	–	–	MeCN	18
24	−0.22	69[c]	–	–	DMF	26
24	−0.18	90[a]	–	–	DMF	27
24	−0.17	80[a]	–	–	MeCN	27
25	+0.01	85[a]	–	–	DMF	27
25	+0.01	85[a]	–	–	MeCN	27
26	+0.19	73[a]	–	–	DMF	27
26	+0.17	81[a]	–	–	MeCN	27
27	+0.21	210[a]	–	–	DMF	27
27	+0.24	112[a]	–	–	MeCN	27
28	−1.01	74[d]	+0.53	75[d]	CH_2Cl_2:DMF(1:1)	28
29	−0.79	65[d]	+0.58	100[d]	CH_2Cl_2:DMF(1:1)	28
30	−0.64	70[d]	+0.70[e]	—	CH_2Cl_2:DMF(1:1)	28

[a]Scan rate 0.2 Vs^{-1}.
[b]Scan rate 0.01 Vs^{-1}.
[c]Scan rate 0.1 Vs^{-1}.
[d]Scan rate not specified.
[e]Peak potential value for irreversible processes.

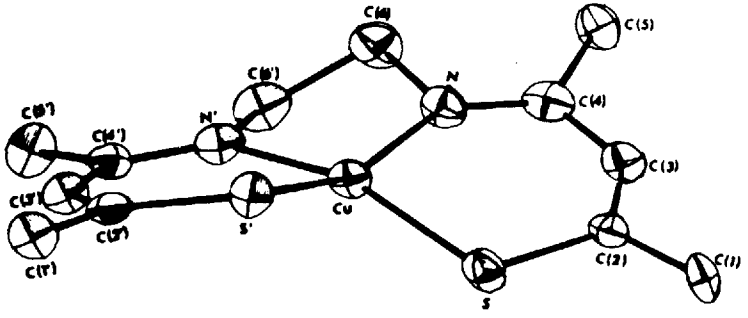

FIGURE 6 Crystal structure of **19**. Cu–S 2.23 Å; Cu–N 1.99 Å (from Ref. 29).

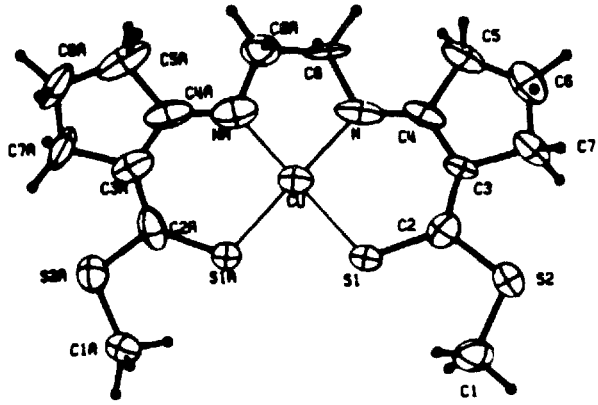

FIGURE 7 Perspective view of **28**. Cu–S 2.25 Å; Cu–N 1.94 Å (from Ref. 30).

On the other hand, **27**, which is surely less flexible than **26**, but contains an electron-withdrawing phenyl group in the N⌐¬N bridge, is even more easily reducible.

The large difference in redox potentials between **22** and **23** is rather disappointing, even considering in **23** both the steric repulsions of methyl groups, which do induce appreciable distortion from planarity, and the presence of a doubly positive charge, which electrostatically favors the addition of electrons. However the redox potential of **23** well fits that of the similar **15**, taking into account the presence of phenyl groups.

Finally, as far as the species **22** is concerned, it is interesting to note that the substitution of the two sulfur atoms for two oxygen atoms shifts the potential of the copper(II)/copper(I) couple towards negative potential values of about 300 mV,[33] as well as the substitution for two NH groups, which leads to a further negative shift of about 400 mV.[25] It is hence evident that the one-electron reduction of copper(II) complexes is facilitated by the presence in the ligands of donor atoms according to the sequence: S > O > N.

Another class of type B complexes is represented by the copper(II) derivatives **31–36**, schematized in Chart V, which present a bridging S⌐¬S carbon chain. As in the preceding cases, the most significant redox change displayed by these complexes is the chem-

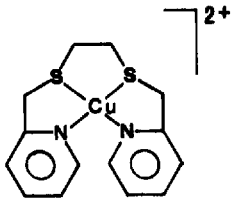

31

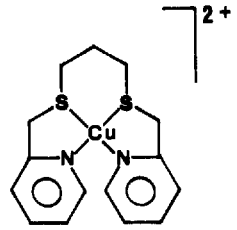

32

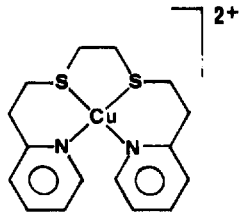

33

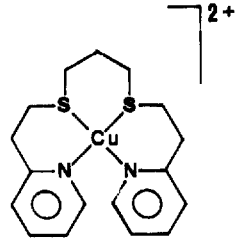

34

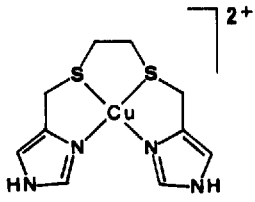

35

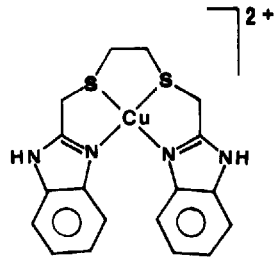

36

CHART V

ically reversible copper(II)/copper(I) reduction. The relevant electrode potentials are reported in Table IV. It is immediately seen that all the complexes present markedly high redox potentials.

As far as the series **31–34** is concerned, it can be noted that the increase of the bridging carbon chain length is accompanied by a progressive destabilization of the copper(II) forms. In donor solvents **31** is assumed to have a square-pyramidal structure, with a solvent molecule occupying a basal position.[34] Unfortunately spectroscopic evidence does not support the simplest hypothesis that the more flexible the ligand becomes with the carbon chain length, the greater is the distortion of the copper(II) coordination from tetragonal to pseudotetrahedral,[34] thus facilitating the access to copper(I). On the other hand, as shown in Fig. 8(a), **33** maintains

TABLE IV

Redox potentials (in volts, vs. S.C.E.) for the copper(II)/copper(I) couple of the complexes **31–36** (schematized in Chart V)

Complexes	$E^{0'}_{Cu^{II}/Cu^{I}}$	ΔE_p (mV)	Solvent	Ref.
31	+0.15	100[a]	H_2O	34
31	+0.49	78[a]	MeCN	34,35
32	+0.23	66[a]	H_2O	34
32	+0.52	70[a]	MeCN	34
32	+0.55	–	MeCN	35
33	+0.53	117[b]	H_2O	36
33	+0.36	87[c]	H_2O	12
33	+0.34	102[a]	H_2O	34
33	+0.38[d]	–	MeCN	21
33	+0.59	84[a]	MeCN	34
34	+0.35	134[a]	H_2O	34
34	+0.40	122[c]	H_2O	12
34	+0.54	90[a]	MeCN	34
34	+0.44	–	MeCN	35
35	+0.23	65[e],140[f]	MeOH	37
35	+0.28	–	MeCN	35
36	+0.34	270[g]	MeCN	38

[a]Scan rate 0.05 Vs^{-1}.
[b]Scan rate 0.02 Vs^{-1}.
[c]Scan rate not specified.
[d]Peak potential value for irreversible process.
[e,f]Different supporting electrolytes.
[g]Scan rate 0.1 Vs^{-1}.

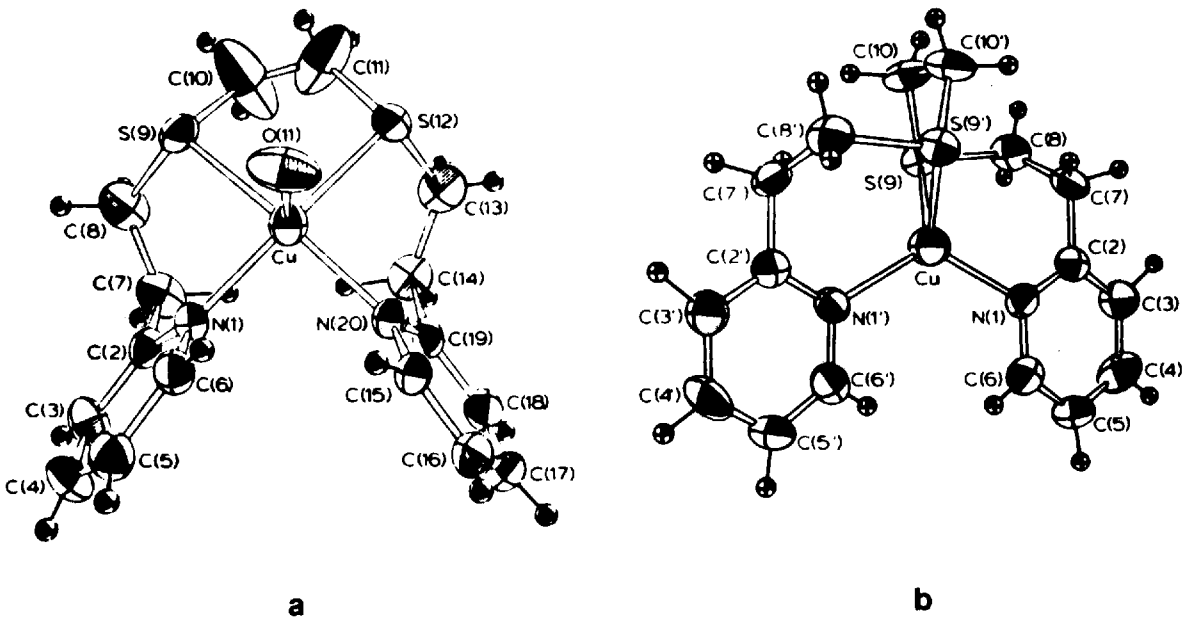

FIGURE 8 (a) Crystal structure of the copper(II) complex **33**. Cu–N 2.01 Å; Cu–S 2.31 Å; Cu–$O_{(ClO_4)}$ 2.26 Å. (b) Crystal structure of the corresponding copper(I) complex. Cu–N 2.04 Å; Cu–S 2.35 Å. Dihedral angle between the CuN_2 and CuS_2 planes 74.5° (from Ref. 36).

in the solid state a square-pyramidal geometry, with the fifth apical position occupied by an oxygen atom of the perchlorate anion. It must be noted that on the contrary the corresponding tetraaza copper(II) complex effectively shows tetrahedral distortion.[39] In this picture, the progressive stabilization of the copper(I) complexes is qualitatively attributed to the fact that the increasing flexibility allows the copper(I) ions to more easily adopt its typical pseudotetrahedral geometry (see Fig. 8(b)).

A tetrahedral distortion from planarity seems to be present in **35**,[37] which however possesses a redox potential lower than that of the same-membered square-pyramidal **31**. This is attributable to the fact that the imidazolyl nitrogen is less a π-acceptor than the pyridyl nitrogen.[35]

Once again it is pointed out that electronic and structural effects concomitantly compete in the location of the copper(II)/copper(I) redox potentials.

In the solid state, a distorted trigonal bipyramidal geometry is assigned to **36**, but it is thought that in solution a change of geometry occurs, likely intermediate between square-pyramidal and trigonal-bipyramidal.[40]

Another series of type B complexes is represented by the copper(II) complexes **37–44**, schematized in Chart VI, having a $\overbrace{N \quad S}$ carbon chain bridge of variable length. These complexes assume different stereochemistries as a function of the flexibility induced by the length of the methylenic chains.[41] Compounds **41**, **42** are stable in nonaqueous solutions for only a few minutes; **43** and **44** even less.[41] As an example, Fig. 9 shows the cyclic voltammogram relevant to the chemically reversible copper(II)/copper(I) reduction of **42** in dimethylformamide solution. Table V summarizes the redox potentials of the quasireversible one-electron reduction of **37–44**.

On the basis of spectroscopic evidence the following redox–structural relationships hold (see also Scheme II). The square-planar complexes **39**, **40** have the lowest redox potentials. Square-pyramidal complexes **37**, **38** appreciably destabilize the copper(II) form, but nearly to the same extent as the trigonal bipyramidal complexes **41**, **42**. Compounds **43**, **44**, which in acetonitrile are likely four-coordinate tetrahedrally distorted, in the more coordinating solvent dimethylformamide are five-coordinate, too; this

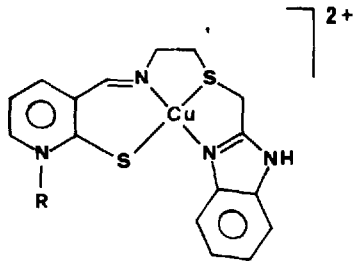

R = C_6H_5 **37**
R = $CH(CH_3)_2$ **38**

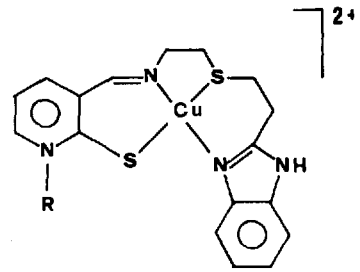

R = C_6H_5 **39**
R = $CH(CH_3)_2$ **40**

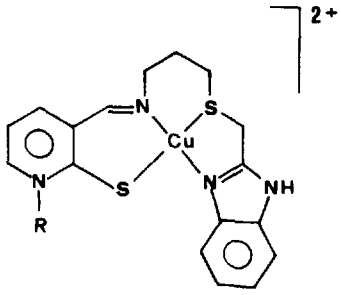

R = C_6H_5 **41**
R = $CH(CH_3)_2$ **42**

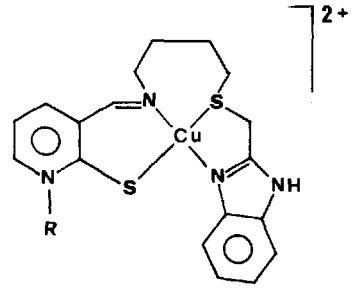

R = C_6H_5 **43**
R = $CH(CH_3)_2$ **44**

CHART VI

explains the fact that their redox potentials are quite comparable to those of **37**, **38** and **41**, **42**.

Assuming a common pseudotetrahedral geometry for all the copper(I) species, we can speculate that in the copper(II)/copper(I) redox change the highest reorganizational barrier is experienced by square planar geometries, whereas five-coordinate square-py-

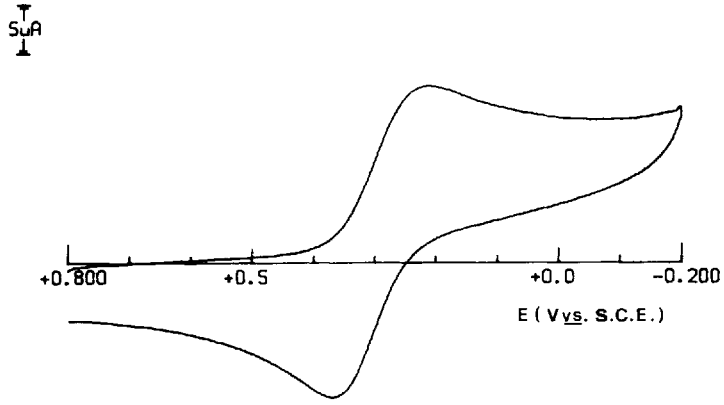

FIGURE 9 Cyclic voltammogram recorded at a platinum electrode on a DMF solution of **42**. Scan rate 0.2 Vs^{-1}.

ramidal or trigonal-bipyramidal assemblies make the reduction step about equally easier. Unfortunately, because of the high instability in acetonitrile of the distorted tetrahedral complexes, we could not prove, as expected, that their redox potentials are the most positive.

TABLE V

Redox potentials (in volts, vs. S.C.E.) for the copper(II)/copper(I) couple of complexes **37–44** (schematized in Chart VI) (Ref. 41)

Complex	$E^{0'}_{CuII/CuI}$	ΔE^{a}_{p} (mV)	Solvent
37	+0.34	118	MeCN
37	+0.34	160	DMF
38	+0.35	80	MeCN
38	+0.33	140	DMF
39	+0.24	108	MeCN
39	+0.24	102	DMF
40	+0.23	122	MeCN
40	+0.24	160	DMF
41	+0.35	127	MeCN
41	+0.32	147	DMF
42	+0.33	100	MeCN
42	+0.30	120	DMF
43	+0.33	200	DMF
44	+0.34	250	DMF

[a]Scan rate 0.2 Vs^{-1}.

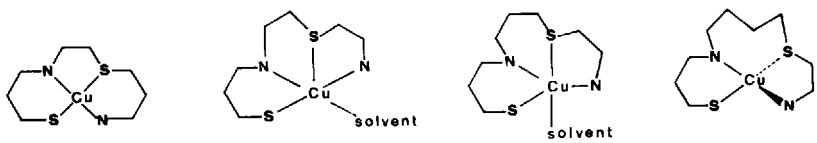

SCHEME II

As last members of type B complexes, we recall some bis(thiosemicarbazone)-copper(II) derivatives, schematized in Chart VII, which attracted attention some years ago. Figure 10, which refers to **46**, exemplifies the redox behavior of these complexes. Neglecting the most positive process likely ligand centered, both the copper(II)/copper(III) oxidation and the copper(II)/copper(I) reduction are displayed.[42] The relevant responses seem to indicate in both cases a chemically reversible process, electrochemically reversible in the case of the oxidation step (ΔE_p = 60 mV), electrochemically quasireversible in the case of the reduction step (ΔE_p = 80 mV).

These copper(II) complexes are thought to be planar by analogy

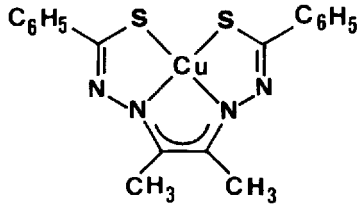

45

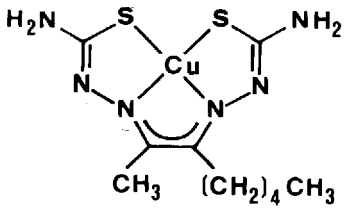

46

CHART VII

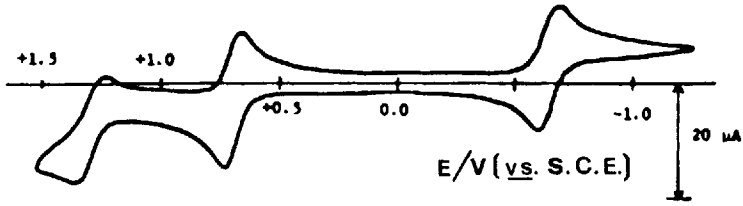

FIGURE 10 Cyclic voltammogram recorded at a platinum electrode on a MeCN solution of **46** (from Ref. 42).

with the crystal structure of 2-keto-3-ethoxybutyraldehyde bis(thiosemicarbazone)-copper(II) species, **47**.[43]

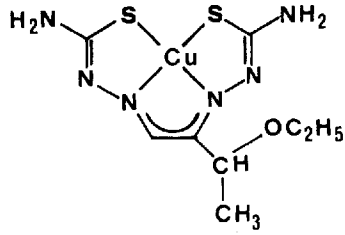

47

Hence, considering that copper(III) complexes are usually planar, the reversibility of the relevant anodic process is not surprising.

Table VI summarizes the redox potentials of the cited redox changes for **45** and **46**. The difference in potential values between the two derivatives are well accounted for by the presence of electron-withdrawing phenyl groups in **45**, which facilitate the electron addition, as well as make difficult the electron removal. In spite of the apparent stability, neither the copper(III) nor the copper(I) complexes could be suitably characterized in such complexes.[42,44]

TABLE VI

Standard electrode potentials (in volts, vs. S.C.E.) for the redox changes of **45** and **46** (schematized in Chart VII)

Complex	$E^{0\prime}_{Cu^{II}/Cu^{I}}$	$E^{0\prime}_{Cu^{II}/Cu^{III}}$	Solvent	Ref.
45	−0.23	–	MeCN	44
45	−0.15	–	DMSO	44
45	−0.09	+1.15	CH_2Cl_2	44
46	−0.64	+0.70	MeCN	42

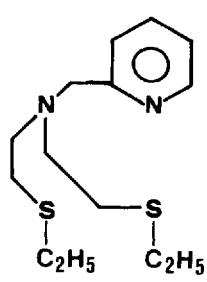

48

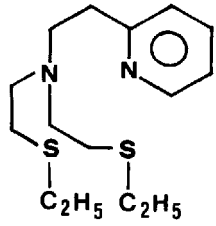

49

CHART VIII

3. Type C Complexes

The tetradentate tripodal ligands **48**, **49**, schematized in Chart VIII, form stable copper(I) complexes. In dimethylformamide solution these copper(I) complexes undergo a quasireversible one-electron oxidation.[45,46] The redox potentials for the relevant copper(I)/copper(II) couples are reported in Table VII.

As shown in Fig. 11, both these copper(I) complexes have a pyramidally distorted tetrahedral geometry. The corresponding copper(II) complexes, both in the solid state and in solution, are five-coordinate, because of their coordination to a counteranion.[46,47] Figure 12 shows the crystal structures of some copper(II)

TABLE VII

Redox potentials (in volts, vs. S.C.E.) for the one-electron oxidation of the copper(I) complexes of the ligands **48**, **49** (schematized in Chart VIII), together with those for the one-electron reduction of the corresponding copper(II) species

Complex	$E^{0\prime}_{Cu^{II}/Cu^{I}}$	Solvent	Ref.
$\|Cu(I)\text{-}\mathbf{48}\|^+$	+0.03	DMF	45,46
$Cu(II)\text{-}\mathbf{48}\text{-}SO_4$	+0.30	aqueous-80% MeOH	48
$\|Cu(II)\text{-}\mathbf{48}\text{-}Cl\|^+$	−0.18	DMF	46
$\|Cu(I)\text{-}\mathbf{49}\|^+$	+0.27	DMF	45,46
$\|Cu(II)\text{-}\mathbf{49}\text{-}NO_3\|^+$	+0.20	DMF	46
$\|Cu(II)\text{-}\mathbf{49}\text{-}Cl\|^+$	+0.04	DMF	46

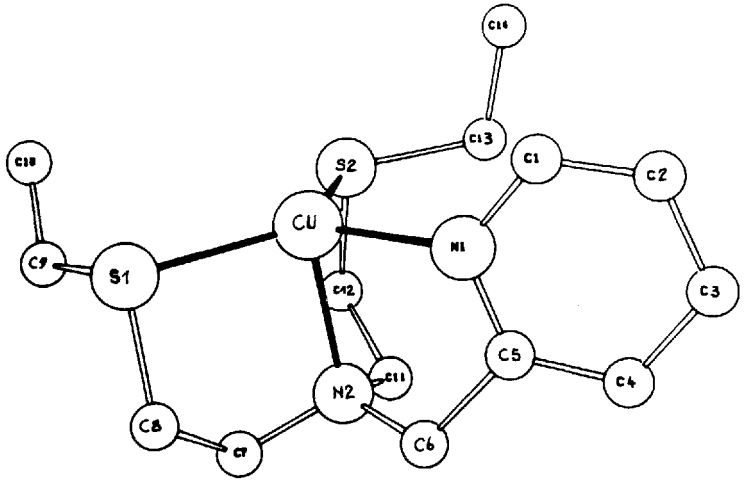

a

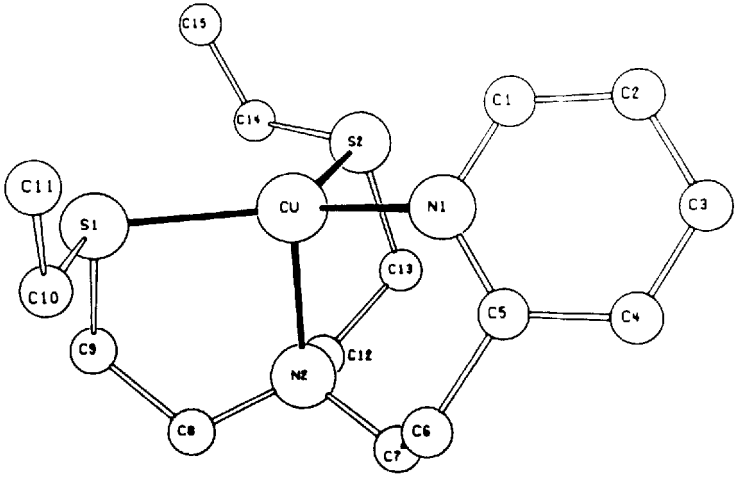

b

FIGURE 11 Crystal structures of: (a) copper(I) complex of **48**. Cu–$N_{(amine)}$ 2.16 Å; Cu–$N_{(pyr)}$ 2.03 Å; Cu–$S_{(mean)}$ 2.25 Å. (b) Copper(I) complex of **49**. Cu–$N_{(amine)}$ 2.19 Å; Cu–$N_{(pyr)}$ 2.00 Å; Cu–$S_{(mean)}$ 2.29 Å (from Ref. 46).

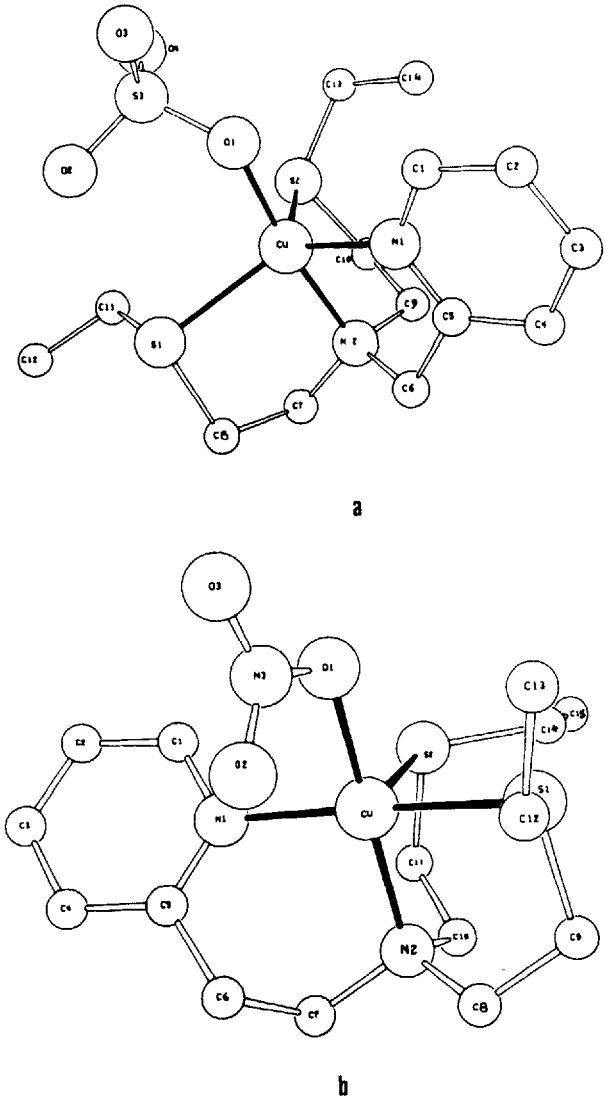

FIGURE 12 Crystal structures of: (a) sulfato-copper(II) complex of **48**. Cu–$N_{(amine)}$ 2.03 Å; Cu–$N_{(pyr)}$ 2.02 Å; Cu–$S_{(mean)}$ 2.42 Å; Cu–O 1.91 Å. (b) Nitrato-copper(II) complex of **49**. Cu–$N_{(amine)}$ 2.08 Å; Cu–$N_{(pyr)}$ 2.03 Å; Cu–$S_{(mean)}$ 2.45 Å; Cu–O 1.99 Å (from Ref. 46).

species of **48** and **49**. It has been pointed out[46] that the relatively small-sized ligand **48**, because of the imposed constraints, gives rise to a trigonal-bipyramidal copper(II) species, whereas the relatively greater-sized ligand **49**, because of the increased flexibility, allows the copper(II) ion to assume a square-pyramidal geometry.

It seems, however, unlikely that these five-coordinate species are the ones instantaneously generated at the electrode surface. In fact, as shown in Table VII, the electrode potentials for the one-electron oxidation of the four-coordinate copper(I) complexes are significantly different from those relative to the one-electron reduction of the corresponding characterized five-coordinate copper(II) species. This seems to suggest that the variation of the coordination number is a reorganizational process *following*, rather than *concomitant* with, the electron removal.

At any rate it is also confirmed in this case that the more flexible the tripodal ligand, the more stable the copper(I) complex.

4. Type D Complexes

The copper(II) complexes **50–62**, schematized in Chart IX, are in principle the ones experiencing minor geometrical constraints, because of the reduced number of linkages connecting the donor atoms. As for most CuN_2S_2 complexes, the most significant redox change is the copper(II)/copper(I) reduction. The relevant redox potentials are summarized in Table VIII.

Among the hitherto examined CuN_2S_2 complexes, **51–55** possess the highest redox potentials. This datum is not easily explainable on the basis of stereochemical arguments. In fact, as shown in Fig. 13, **53** has an elongated octahedral geometry with a strictly planar CuN_2S_2 moiety.[35] The same geometry, widely accepted to destabilize copper(I) complexes, is typical for complexes **56–59**,[37] which also display rather high redox potentials. As a further apparent contradiction, the more electrondonating is the substituent R in **51–55** (as, on the other hand, in **56–59**), the easier is the addition of electrons.

Really none of the usual arguments (electronic and/or stereochemical effects) seems well suited to prelude the absolute location of these redox potentials. We can speculate that, once the reduced copper(I) species have lost the axially bound anions, they have no bridging chain between the two wings, which may reduce their

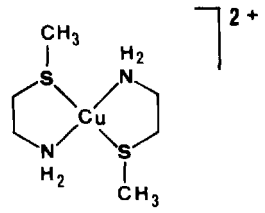

50

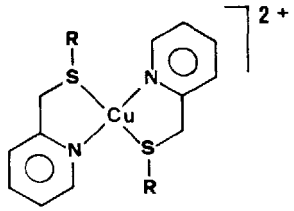

R = CH_3 **51**
R = C_2H_5 **52**
R = $n-C_3H_7$ **53**
R = $t-C_4H_9$ **54**
R = $CH_2-C_6H_5$ **55**

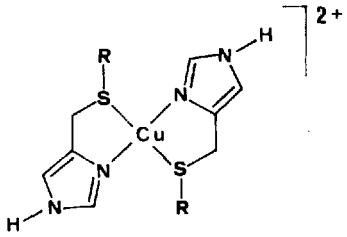

R = $n-C_3H_7$ **56**
R = $t-C_4H_9$ **57**
R = C_6H_5 **58**
R = $CH_2-C_6H_5$ **59**

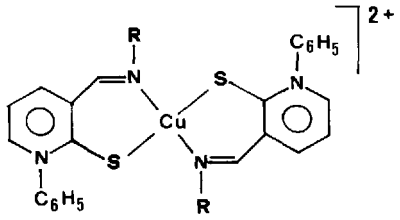

R = s—C_4H_9
R = p—CH_3—C_6H_4
R = m—NO_2—C_6H_4

CHART IX

attitude to assume a tetrahedral geometry, as, on the contrary, occurs to some extent for all the previously examined complexes.

The progressive increase of redox potentials passing from **50** to **56–59** to **51–55** has been attributed to the π-accepting ability of

TABLE VIII

Redox potentials (in volts, vs. S.C.E.) for the copper(II)/copper(I) couple of the complexes **50–62** (schematized in Chart IX)

Complex	$E^{0'}_{CuII/CuI}$	ΔE_p (mV)	Solvent	Ref.
50	+0.33	–	MeCN	35
51	+0.66	–	MeCN	35
52	+0.68	–	MeCN	35
53	+0.69	–	MeCN	35
54	+0.73	–	MeCN	35
55	+0.72	–	MeCN	35
56	+0.37	–	MeCN	35
56	+0.33[a]	60[b]	MeOH	37
56	+0.28[c]	110[b]	MeOH	37
57	+0.43	–	MeCN	35
57	+0.37[a]	85[b]	MeOH	37
57	+0.35[c]	300[b]	MeOH	37
58	+0.36[a]	100[b]	MeOH	37
58	+0.32[c]	100[b]	MeOH	37
59	+0.41	–	MeCN	35
59	+0.34[a]	60[b]	MeOH	37
59	+0.30[c]	130[b]	MeOH	37
60	+0.55	270[d]	MeCN	27
61	+0.43	81[d]	MeCN	27
62	+0.56	86[d]	MeCN	27

[a] $|NBu_4|BF_4$ supporting electrolyte.
[b] Scan rate 0.1 Vs^{-1}.
[c] $|NBu_4|ClO_4$ supporting electrolyte.
[d] Scan rate 0.2 Vs^{-1}.

the nitrogen atoms which increases according to the sequence: amino < imidazolyl < pyridyl.[35]

In Table VIII a curious aspect of the reduction of complexes **56–59** is also outlined. In the presence of different supporting electrolytes ($|NBu_4|BF_4$ or $|NBu_4|ClO_4$), not only slight variations of redox potentials occur (which is enough of a common feature of electrode processes), but the extent of electrochemical reversibility appears constantly lower in the presence of $|NBu_4|ClO_4$. It would be suggestive to correlate this likely higher reorganizational barrier to the electron transfer with the difficulty to remove from the six-coordinate copper(II) species, during the reduction to four-coordinate copper(I) species, the apical bound ClO_4 molecules in the presence of a large excess of perchlorate ions.

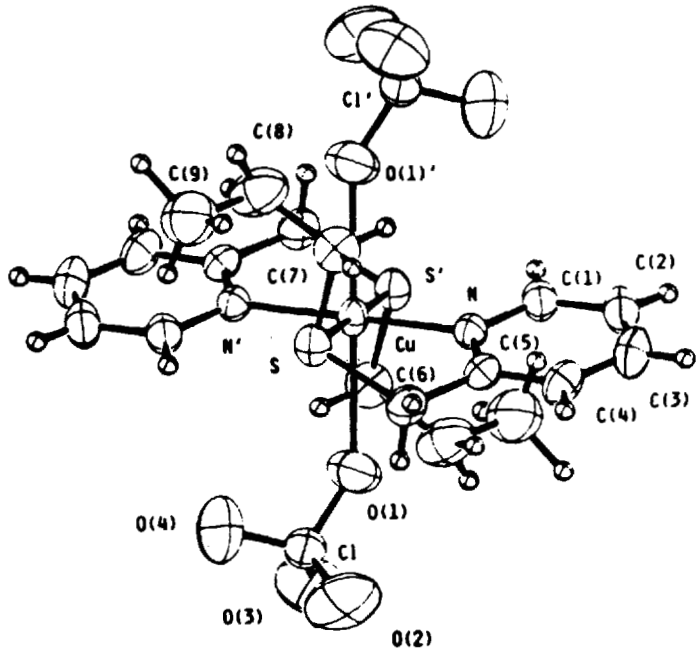

FIGURE 13 Molecular structure of the copper(II) complex **53**. Cu–S 2.37 Å; Cu–N 2.01 Å; Cu–O 2.50 Å (from Ref. 35).

Finally, spectroscopic evidence assigns tetrahedral distortions to complexes **60–62**,[32] thus rationally explaining their notably higher redox potentials, too.

CONCLUDING REMARKS

Many CuN_2S_2 complexes constitute valid models of blue copper proteins also because they display high reduction potentials. It is here pointed out that two main sources can concomitantly compete in originating markedly positive redox potentials: (i) flexible ligand designs, which allow copper(II) or copper(I) centers to rearrange easily to the tetrahedral geometry typical for copper(I) complexes; (ii) electron-withdrawing overall effects of the ligand functions,

which, depleting the electron density on the metal, favor the addition of electrons. Congruent and incongruous relationships have been shown. However, also because of the well-known redox instability of copper(II) oxidation state towards thiolate bonding (see references cited in Ref. 41), too few copper(II)/copper(I) redox couples have been structurally characterized, both in the solid state and in solution, to permit a more detailed correlation between structural reorganizations and electrochemical parameters, other than the qualitative, and often speculative, arguments now unavoidably invoked.

Abbreviations for Solvents

DMF	N,N-Dimethylformamide
DMSO	Dimethyl sulfoxide
MeCN	Acetonitrile
MeOH	Methanol
PC	Propylene carbonate

References

1. A. J. Fee, Struct. Bonding (Berlin) **23**, 1 (1975).
2. T. G. Spiro (Ed.), *Copper Proteins* (Wiley Interscience, New York, 1981).
3. K. D. Karlin and J. Zubieta (Eds.), *Copper Coordination Chemistry: Biochemical and Inorganic Perspectives* (Adenine Press, Guilderland, N.Y., 1983).
4. K. D. Karlin and J. Zubieta (Eds.), *Biological and Inorganic Copper Chemistry* (Adenine Press, Guilderland, N.Y., 1986).
5. P. M. Colman, H. C. Freeman, J. M. Guss, M. Murata, V. A. Norris, J. A. M. Ramshaw and M. P. Venkatappa, Nature **272**, 319 (1981).
6. K. W. Penfield, R. R. Gay, R. S. Himmelwright, N. C. Eickman, V. A. Norris, H. C. Freeman and E. I. Solomon, J. Am. Chem. Soc. **103**, 4382 (1981).
7. G. E. Norris, B. F. Anderson and E. N. Baker, J. Am. Chem. Soc. **108**, 2784 (1986).
8. P. Zanello, S. Tamburini, P. A. Vigato and G. A. Mazzocchin, Coord. Chem. Rev. **77**, 165 (1987).
9. B. Reinhammar and B. Malmström, in Ref. 2, p. 109.
10. M. A. Augustin, J. K. Yandell, A. W. Addison and K. D. Karlin, Inorg. Chim. Acta **55**, L35 (1981), and references therein.
11. W. E. Geiger, Progr. Inorg. Chem. **33**, 275 (1985).
12. D. B. Rorabacher, M. J. Martin, M. J. Koenigbauer, M. Malik, R. R. Schroeder, J. F. Endicott and L. A. Ochrymowycz, in Ref. 3, p. 167.
13. J. P. Gisselbrecht and M. Gross, in *Advances in Chemistry Series, No. 201.*

Electrochemical and Spectrochemical Studies of Biological Redox Components, ed. K. M. Kadish (Am. Chem. Soc., 1982), p. 109.
14. L. Siegfried and T. A. Kaden, Helv. Chim. Acta **67**, 29 (1984).
15. K. P. Balakrishnan, T. A. Kaden, L. Siegfried and A. D. Zuberbühler, Helv. Chim. Acta **67**, 1061 (1984).
16. E. R. Brown and J. R. Sandifer, in *Physical Methods of Chemistry. Electrochemical Methods*, eds. B. W. Rossiter and J. F. Hamilton (J. Wiley, New York, 1986), Vol. 2, Chapt. 4.
17. L. Fabbrizzi, A. Poggi and P. Zanello, J. Chem. Soc., Dalton Trans. 2191 (1983).
18. A. W. Addison, T. N. Rao and E. Sinn, Inorg. Chem. **23**, 1957 (1984).
19. T. A. Kaden, S. Kaderli, W. Sager, L. C. Siegfried-Hertli and A. D. Zuberbühler, Helv. Chim. Acta **69**, 1217 (1986).
20. E. R. Dockal, T. E. Jones, W. F. Sokol, R. J. Engerer, D. B. Rorabacher and L. A. Ochrymowycz, J. Am. Chem. Soc. **98**, 4322 (1976).
21. U. Sakaguchi and A. W. Addison, J. Chem. Soc., Dalton Trans. 600 (1979).
22. L. Fabbrizzi, A. Poggi and P. Zanello, J. Chem. Soc., Dalton Trans. 1495 (1984).
23. A. Cinquantini, R. Cini, R. Seeber and P. Zanello, J. Electroanal. Chem. **121**, 301 (1981).
24. W. R. Pangratz, F. L. Urbach, P. R. Blum and S. C. Cummings, Inorg. Nucl. Chem. Letters **9**, 1141 (1973).
25. G. S. Patterson and R. H. Holm, Bioinorg. Chem. **4**, 257 (1975).
26. J. Becher, D. J. Brockway, K. S. Murray, P. J. Newman and H. Toftlund, Inorg. Chem. **21**, 1791 (1982).
27. P. Zanello, L. Casella and M. Gullotti, work in progress.
28. J. R. Dorfman, R. D. Bereman and M.-H. Whangbo, in Ref. 3, p. 75.
29. R. Cini, A. Cinquantini, P. Orioli and M. Sabat, Cryst. Struct. Comm. **9**, 865 (1980).
30. R. D. Bereman, J. R. Dorfman, J. Bordner, D. P. Rillema, P. McCarthy and G. D. Shields, J. Inorg. Biochem. **16**, 47 (1982).
31. M. F. Corrigan, K. S. Murray, B. O. West and J. R. Pilbrow, Aust. J. Chem. **30**, 2455 (1977).
32. L. Casella, M. Gullotti and R. Viganò, Inorg. Chim. Acta **124**, 121 (1986).
33. P. Zanello and A. Cinquantini, Transition Metal Chem. **10**, 370 (1985).
34. D. E. Nikles, M. J. Powers and F. L. Urbach, Inorg. Chem. **22**, 3210 (1983).
35. N. Aoi, G.-E. Matsubayashi, T. Tanaka and K. Nakatsu, Inorg. Chim. Acta **85**, 123 (1984).
36. G. R. Brubaker, J. N. Brown, M. K. Yoo, R. A. Kinsey, T. M. Kutchan and E. A. Mottel, Inorg. Chem. **18**, 299 (1979).
37. N. Aoi, G.-E. Matsubayashi and T. Tanaka, J. Chem. Soc., Dalton Trans. 1059 (1983).
38. M. F. Cabral, J. De O. Cabral, J. Van Rijn and J. Reedijk, Inorg. Chim. Acta **87**, 87 (1984).
39. D. A. Wright and J. D. Quinn, Acta Crystallogr., Sect. B. **30**, 2132 (1974).
40. P. J. M. W. L. Birker, J. Helder, G. Henkel, B. Krebs and J. Reedijk, Inorg. Chem. **21**, 357 (1982).
41. L. Casella, M. Gullotti, A. Pintar, F. Pinciroli, R. Viganò and P. Zanello, submitted.
42. L. E. Warren, S. M. Horner and W. E. Hatfield, J. Am. Chem. Soc. **94**, 6392 (1972).

43. M. R. Taylor, E. J. Gabe, J. P. Glusker, J. A. Minkin and A. L. Patterson, J. Am. Chem. Soc. **88**, 1845 (1966).
44. R. H. Holm, A. L. Balch, A. Davison, A. H. Maki and T. E. Berry, J. Am. Chem. Soc. **89**, 2866 (1967).
45. K. D. Karlin and S. E. Sherman, Inorg. Chim. Acta **65**, L39 (1982).
46. J. Zubieta, K. D. Karlin and J. C. Hayes, in Ref. 3, p. 97.
47. K. D. Karlin and J. K. Yandell, Inorg. Chem. **23**, 1184 (1984).
48. K. D. Karlin, P. L. Dahlstrom, J. R. Hyde and J. Zubieta, J. Chem. Soc., Chem. Commun. 906 (1980).